• Clinical Research •

# Evaluation of corneal topographic, tomographic and biomechanical indices for detecting clinical and subclinical keratoconus: a comprehensive three-device study

*Zahra Heidari*[1,2], *Hassan Hashemi*[1], *Mehrdad Mohammadpour*[1,3], *Kazem Amanzadeh*[4], *Akbar Fotouhi*[5]

[1]Noor Ophthalmology Research Center, Noor Eye Hospital, Tehran 1968653111, Iran
[2]School of Medicine, Tehran University of Medical Sciences, Tehran 1417613151, Iran
[3]Department of Ophthalmology, Farabi Eye Hospital and Eye Research Center, Faculty of Medicine, Tehran University of Medical Sciences, Tehran 1336616351, Iran
[4]Noor Research Center for Ophthalmic Epidemiology, Noor Eye Hospital, Tehran 1968653111, Iran
[5]Department of Epidemiology and Biostatistics, School of Public Health, Tehran University of Medical Sciences, Tehran 1417613151, Iran
**Correspondence to:** Mehrdad Mohammadpour. Department of Ophthalmology, Farabi Eye Hospital and Eye Research Center, Faculty of Medicine, Tehran University of Medical Sciences, Tehran 1336616351, Iran. mahammadpour@yahoo.com
Received: 2020-03-12 Accepted: 2020-09-16

## Abstract

● **AIM:** To evaluate the diagnostic ability of topographic and tomographic indices with Pentacam and Sirius as well as biomechanical parameters with Corvis ST for the detection of clinical and subclinical forms of keratoconus (KCN).

● **METHODS:** In this prospective diagnostic test study, 70 patients with clinical KCN, 79 patients with abnormal findings in topography and tomography maps with no evidence on clinical examination (subclinical KCN), and 68 normal control subjects were enrolled. The accuracy of topographic, tomographic, and biomechanical parameters was evaluated using the area under the receiver operating characteristic curve (AUC) and cross-validation analysis. The Delong method was used for comparing AUCs.

● **RESULTS:** In distinguishing KCN from normal, all parameters showed statistically significant differences between the two groups ($P$<0.001). Indices with the perfect diagnostic ability (AUC≥0.999) were Sirius KCN vertex of back (KVb), Pentacam random forest index (PRFI), Pentacam index of height decentration (IHD), and Corvis integrated tomographic/biomechanical index (TBI). In distinguishing subclinical KCN from normal, Sirius symmetry index of back (SIb; AUC=0.908), Pentacam inferior-superior difference (IS) value (AUC=0.862), PRFI (AUC=0.847), and Corvis TBI (AUC=0.820) performed best. There were no significant differences between the highest AUCs within keratoconic groups (DeLong, $P$>0.05).

● **CONCLUSION:** In clinical KCN, all topographic, tomographic, and biomechanical indices have acceptable outcomes in terms of sensitivity and specificity. However, in differentiating subclinical forms of KCN from normal corneas, curvature-based parameters (SIb and IS value) followed by integrated indices (PRFI and TBI) are the most powerful tools for early detection of KCN.

● **KEYWORDS:** topography; tomography; biomechanical index; keratoconus; subclinical keratoconus

**DOI:10.18240/ijo.2021.02.08**

**Citation:** Heidari Z, Hashemi H, Mohammadpour M, Amanzadeh K, Fotouhi A. Evaluation of corneal topographic, tomographic and biomechanical indices for detecting clinical and subclinical keratoconus: a comprehensive three-device study. *Int J Ophthalmol* 2021;14(2):228-239

## INTRODUCTION

Keratoconus (KCN) is an ectatic condition of the cornea that can be detected through routine clinical examinations in advanced stages. In the early stages, however, patients may appear normal in visual acuity and slit-lamp examinations, and thus, diagnosis relies on a thorough assessment of topographic and tomographic images which can show subtle changes in corneal thickness and regularity[1] and it may lead to proper patient detection for the early management of KCN[2].

Pentacam HR (Oculus Optikgeräte GmbH, Wetzlar, Germany) is one of the most commonly used topography and tomography systems that utilizes a rotating Scheimpflug camera and a monochromatic slit-light source to take 100 slit images from 0 to 360°. These images, which are captured in 2s, provide data for 25 000 elevation points that are used for creating a 3D representation of the anterior segment, including the anterior and posterior cornea.

Sirius (Costruzione Strumenti Oftalmici, Florence, Italy) is another device that combines Scheimpflug tomography with Placido-disk topography and analyzes more than 100 000 points to provide comprehensive information about the cornea through the Phoenix software. Studies on the agreement between Pentacam and Sirius in terms of topographic and pachymetric measurements have arrived at inconsistent results[3-5].

Corneal biomechanical properties are other parameters that can be helpful in detecting KCN in its early stages[6]. Corvis ST (Oculus Optikgeräte GmbH, Wetzlar, Germany) is a non-contact air-puff tonometer that integrates Pentacam data to perform a combined tomographic and biomechanical analysis with acceptable reliability[7-8]. It uses a high-speed Scheimpflug camera which takes 4000 frames/second from ocular movements and records corneal deformation responses.

In recent years, new integrated indices have been introduced that offer a high diagnostic ability for KCN[6,9-10]. However, the detection of subclinical KCN (SKCN) cases is still challenging. This study was conducted to identify the most powerful topographic, tomographic, and biomechanical indices for the detection of KCN and SKCN.

## SUBJECTS AND METHODS

**Ethical Approval** This study was approved by the Ethics Committee of Tehran University of Medical Sciences and was conducted at Noor Eye Hospital, Tehran, Iran from April to December 2018. All study procedures were in accordance with the Declaration of Helsinki and written informed consent was obtained from all participants prior to enrollment.

**Study Groups** For this study, participants were recruited from patients referred to the KCN Clinic and individuals undergoing preoperative workup at the Refractive Surgery Unit. Based on findings in their clinical examinations and Pentacam topographic data, they were assigned by an experienced corneal specialist (Amanzadeh K) to one of the following groups: 1) KCN: Inclusion criteria for this group were scissoring on retinoscopy, at least one definitive sign of KCN on clinical examination, including Fleisher rings, Vogt's striae, apical thinning, Munson's sign, or Rizzuti's sign[11], and abnormal topographic criteria such as skewed asymmetric bow tie, central or inferior steepening or a claw pattern on topography, skewed radial axis (SRAX)>20 degrees, max keratometry ($K_{max}$)>48.7 D, and inferior-superior difference value (I-S value)>1.9 D at 6 mm (3 mm radii)[12]; 2) SKCN: Inclusion criteria for this group were no scissoring on retinoscopy, no abnormal findings on slit-lamp biomicroscopy, and presence of abnormal topographic criteria including skewed asymmetric bow tie, central or inferior steepening, 0<SRAX<20 degrees, 47.2<$K_{max}$<48.7 D, and 1.4<I-S value<1.9 D at 6 mm (3 mm radii), and abnormal elevation values on the anterior and posterior elevation maps[12-13]. Eyes with normal-appearing cornea on slit-lamp biomicroscopy, keratometry, retinoscopy, and ophthalmoscopy with inferior-superior asymmetry, bow-tie pattern and skewed radial axis and no history of contact lens use, ocular surgery, or trauma were considered as SKCN[14]; 3) Normal: Eyes included in this group were refractive surgery candidates with normal clinical evaluation based on slit-lamp biomicroscopy and retinoscopy and no abnormal topographic criteria.

Exclusion criteria were any previous ocular surgery or trauma, presence of a corneal scar, hydrops or opacity, dry eye, history of contact lens wear, connective tissue disease, any systemic disease affecting the eyes, use of special medications, ocular or systemic allergic conditions, and pregnancy. If both eyes met the inclusion criteria, only one eye was randomly selected to avoid the effect of fellow eye correlations.

**Ocular Measurements** All participants underwent clinical examinations including retinoscopy, slit-lamp biomicroscopy, and fundoscopy. The amounts of sphere and cylinder were measured using manifest refraction. Then, the best-corrected visual acuity (BCVA) was measured using a Snellen chart and recorded in logMAR. Finally, imaging was done with Pentacam, Sirius, and Corvis ST. Measurement repeatability with the Pentacam, Sirius, and Corvis ST have been reported in normal and KCN eyes, previously[4,15]. The patients were asked to fixate on the central target in all imaging steps and not to blink during the Scheimpflug camera rotation. Images with acceptable quality (quality specifications=OK) were selected. All measurements were done between 9:00 *a.m.* and 4:00 *p.m.* by an expert operator during one visit.

**Topographic, Tomographic, and Biomechanical Parameters** Variables extracted from Pentacam (software version 1.22r03) were curvature-based, elevation based, pachymetric, and integrated indices. Curvature based parameters included front and back corneal surfaces keratometry at 3 mm of the cornea (flat=K1, and steep=K2), $K_{max}$ at the front/back corneal surface, anterior and posterior average radius of curvature in the 3 mm zone (ARC, PRC), and the index of surface variance (ISV), index of vertical asymmetry (IVA), KCN index (KI), central KCN index (CKI), I-S value and KCN percentage index (KISA). Index of height asymmetry (IHA), index of height decentration (IHD) were included as elevation based data.

Pachymetric indices included the thinnest corneal point (TCP), maximum pachymetric progression index ($PPI_{max}$), Ambrosio's relational thickness maximum ($ART_{max}$, which is calculated by dividing the thinnest pachymetry value by the maximum pachymetric progression). Belin/Ambrosio enhanced ectasia total deviation value (BADD) and Pentacam random forest index (PRFI) included as integrated indices.

**Table 1 Demographic characteristics of participants in normal, SKCN, and KCN groups** mean±SD (range)

| Eyes (*n*) | Normal (*n*=68) | SKCN (*n*=79) | KCN (*n*=70) | Total (*n*=217) | $P^1$ | $P^2$ |
|---|---|---|---|---|---|---|
| Age (y) | 30.7±7.01 (19-49) | 30.15±5.42 (17-42) | 32.5±6.07 (18-47) | 31.08±6.21 (17-49) | 1.000 | 0.267 |
| Sphere (D) | -2.30±2.17 (-6.00 to +8.00) | -1.69±2.04 (-8.75 to +2.5) | -2.33±3.01 (-13.5 to +3.75) | -2.09±2.47 (-13.5 to +8.00) | 0.406 | 1.000 |
| Cylinder (D) | -1.63±1.58 (0.0 to -7.25) | -1.44±1.17 (0 to -5.00) | -3.34±1.88 (-0.50 to -10.75) | -2.11±1.76 (0 to -10.75) | 1.000 | <0.001 |
| SE (D) | -1.48±2.48 (-5.50 to +8.88) | -0.96±2.12 (-8.25 to +2.75) | -0.65±3.05 (-11.50 to +6.38) | -1.03±2.57 (-11.50 to +8.88) | 0.673 | 0.183 |
| BCVA, logMAR | 0.01±0.04 (0 to +0.2) | 0.03±0.02 (0 to +0.3) | 0.32±0.21 (0.1 to +0.8) | 0.11±0.19 (0 to +0.8) | 1.000 | <0.001 |

D: Diopters; SE: Spherical equivalent; BCVA: Best-corrected visual acuity; logMAR: Logarithm of the minimum angle of resolution; SKCN: Subclinical keratoconus; KCN: Keratoconus. [1]The comparison between normal and SKCN eyes; [2]The comparison between normal and KCN eyes (ANOVA/Bonferroni).

The extracted parameters from Sirius (Phoenix software version 3.4.0.73) were curvature-based parameters such as K1 and K2 of SimK, max keratometry (Curv), symmetry index of front and back of corneal curvature (SIf and SIb), and an elevation based parameters such as KCN vertex front/back (KVf and KVb). The thinnest corneal thickness (Thk-Min) included as a pachymetric index.

Parameters extracted from Corvis ST (software version 1.6r2031) were deformation parameters, deflection parameters, and integrated indices. Deformation parameters included length of the flattened cornea at first/second applanations (A1L, A2L), time from the beginning of air-puff until the first/second applanation (A1T, A2T), corneal velocity at the first/second applanations (A1V, A2V), deformation amplitude ratio at 1 mm and 2 mm (DAratio1, DAratio2), deformation amplitude at the moment of highest concavity (HCDA). Deflection parameters included deflection amplitude of the first/second applanation (A1DfA, A2DfA), deflection amplitude of the highest concavity (HCDfA), max inverse radius (InvRadMax), and integrated radius (IntRC1). Corvis ST integrated indices included Ambrosio relational thickness to the horizontal profile (ARTh=CT thinnest/Pachymetric progression)[16], Stiffness parameter at first applanation (SPA1) [adjusted pressure at A1 (adj AP1)-bIOP]/A1DeflAmp][10], Corneal biomechanical index (CBI)[6], and the topographic and biomechanical index (TBI)[9].

Figure 1 shows samples of the biomechanical and tomographic maps from Sirius, Pentacam, and Corvis in the SKCN eye.

**Data Analysis** SPSS software (version 23; IBM Inc., New York, NY, USA) was used for data analysis. Descriptive analysis was performed in all groups, and then the mean values of the parameters were compared between the three groups using one-way analysis of variance (ANOVA). Bonferroni multiple comparison correction was applied to compare SKCN and KCN groups with the normal group. Receiver operating characteristic (ROC) curve analysis was performed for all variables to determine the area under the ROC curve (AUC) and describe the discriminative ability of various variables. An AUC of 1.00 indicates perfect discrimination ability.

The optimum cutoff values were determined using the Youden index, and then sensitivity [true positive/(true positive+false negative)]; specificity [true negative/(true negative+false positive)]; positive likelihood ratio [sensitivity/(1-specificity)], negative likelihood ratio [(1-sensitivity)/specificity] were reported for variables with the highest AUCs. A pairwise comparison with the DeLong[17] method was applied to compare ROC curves. The relationship between the variables with the highest AUCs was evaluated with the Pearson correlation test. *P* values less than 0.05 were considered statistically significant.

In addition, the repeated cross-validation analysis was performed to evaluate the prediction capability of clinical parameters with the highest diagnostic power by 'ROCR' and 'crossval' packages using R software, version 3.6.3 (R Foundation for Statistical Computing, Vienna, Austria).

## RESULTS

A total of 217 eyes (70 KCN, 79 SKCN, and 68 normal eyes) were enrolled in this study. Females accounted for 63.0% of normal subjects, whereas 60.0% of the keratoconic patients were male. A summary of the demographic characteristics of each group is presented in Table 1.

**Keratoconus Versus Normal** Topographic, tomographic, and biomechanical variables of the normal and KCN groups are shown in Table 2. All parameters were significantly different between the normal and KCN groups ($P$<0.001). Table 3 shows the results of ROC curve analyses for the ability of studied parameters to differentiate KCN from normal corneas.

In discriminating KCN from normal eyes, the Corvis TBI (with cutoff of 0.80) provided 100% sensitivity and 100% specificity with perfect AUC (1.00). The Sirius KVb (sensitivity 100%, specificity 98.5%, and AUC 0.999) and Pentacam PRFI (sensitivity 99.2%, specificity 100%, and AUC 1.00) followed by Pentacam IHD (sensitivity 98.6%, specificity 100% and AUC 0.999) had the highest diagnostic ability (Delong, $P$>0.05).

The results of cross-validation analysis were compatible with diagnostic evaluation with ROC curve analysis for identifying

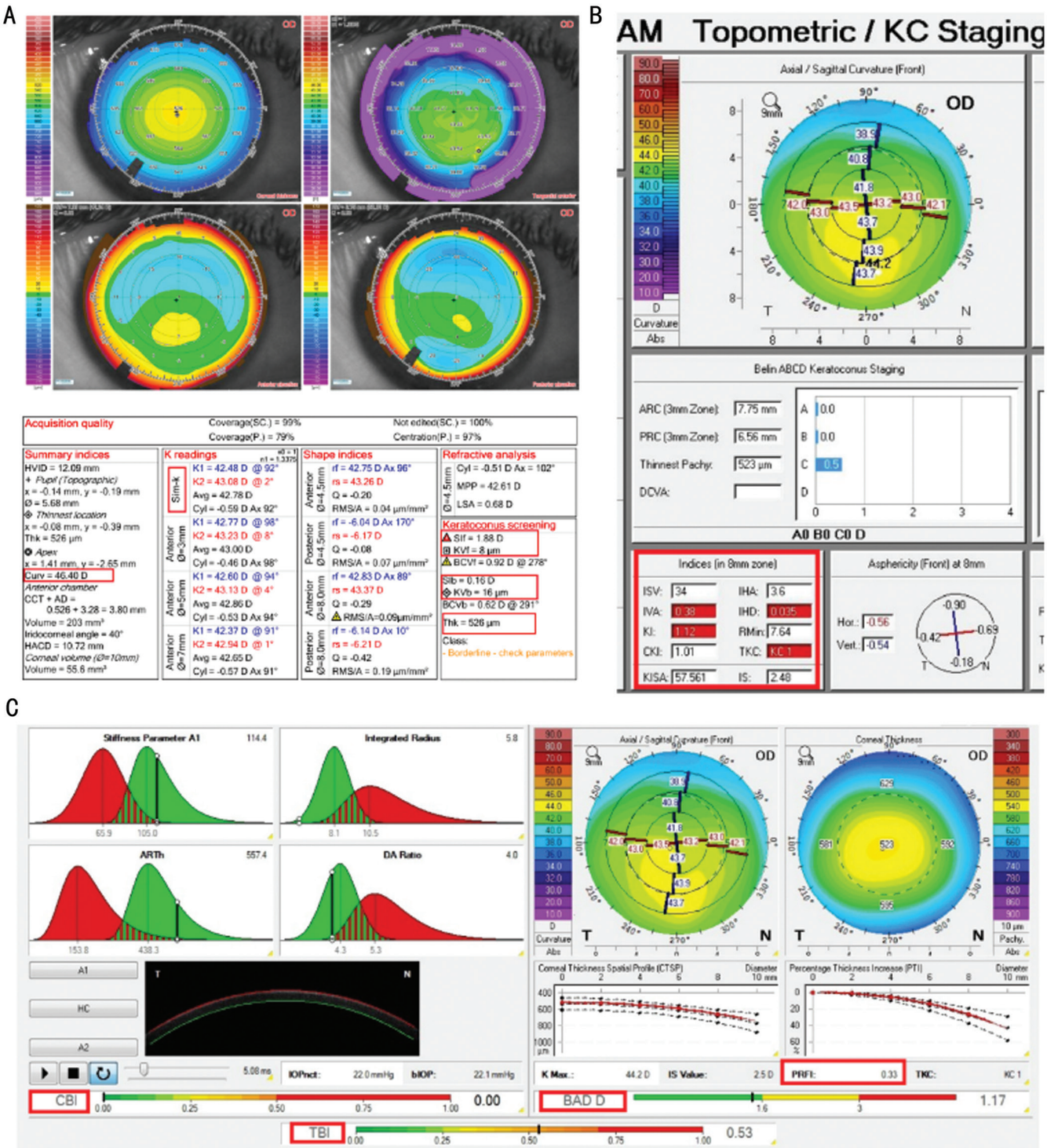


**Figure 1 A samples of the biomechanical and tomographic maps with Sirius (A), Pentacam (B), and Corvis (C) including Curv, SIf and SIb, KVf and KVb and Thk-Min of Sirius, and ISV, IVA, KI, CKI, IS value and KISA, IHA, IHD, BADD and PRFI of Pentacam, and CBI, and TBI of Corvis on the right eye of a patient with SKCN.**

indices with the highest diagnostic ability for KCN (Table 4). There were significant positive correlations between the parameters with the highest AUCs (all correlations were between 0.7 to 0.9, and $P$<0.001). The correlations between KVb and IHD, and between PRFI and TBI were strong ($r$=0.95, $P$<0.001).

**Subclinical Keratoconus Versus Normal** Topographic, tomographic, and biomechanical variables of the normal and SKCN groups are shown in Table 2. Comparison of curvature based parameters between SKCN and control groups showed significant differences for four parameters of Pentacam (PRC, IVA, KI, and IS value), and two parameters of Sirius (SIf and Sib; $P$<0.05). Also, there was a statistically significant difference in elevation based and integrated parameters between SKCN and normal groups ($P$<0.05) and all pachymetric indices of both devices ($P$<0.001). Comparison of

**Table 2 Mean range of the studied parameters in normal, SKCN, and KCN eyes**

| Parameters | Normal | SKCN | KCN | *P* (ANOVA) | $P^1$ | $P^2$ |
|---|---|---|---|---|---|---|
| Pentacam | | | | | | |
| Curvature based | | | | | | |
| Front K1 (D) | 42.972±1.538 | 43.122±1.718 | 45.697±2.745 | <0.001 | NS | <0.001 |
| Front K2 (D) | 44.654±1.695 | 44.681±1.894 | 49.036±3.317 | <0.001 | NS | <0.001 |
| Front $K_{max}$ (D) | 45.062±1.754 | 45.826±2.077 | 53.795±4.642 | <0.001 | NS | <0.001 |
| Back K1(D) | -6.075±0.248 | -6.110±0.300 | -6.684±0.630 | <0.001 | NS | <0.001 |
| Back K2 (D) | -6.519±0.306 | -6.527±0.349 | -7.374±0.675 | <0.001 | NS | <0.001 |
| Back $K_{max}$ (mm) | -6.290±0.255 | -6.306±0.302 | -7.001±0.626 | <0.001 | NS | <0.001 |
| ARC (mm) | 7.707±0.261 | 7.613±0.314 | 6.817±0.472 | <0.001 | NS | <0.001 |
| PRC (mm) | 6.278±0.253 | 6.100±0.326 | 5.188±0.487 | <0.001 | 0.012 | <0.001 |
| ISV | 19.632±8.197 | 26.114±10.131 | 72.814±30.621 | <0.001 | NS | <0.001 |
| IVA | 0.109±0.041 | 0.227±0.132 | 0.784±0.413 | <0.001 | 0.013 | <0.001 |
| KI | 1.021±0.019 | 1.055±0.032 | 1.200±0.106 | <0.001 | 0.005 | <0.001 |
| CKI | 1.007±0.005 | 1.009±0.011 | 1.047±0.037 | <0.001 | NS | <0.001 |
| I-S value (D) | 0.122±0.530 | 1.275±0.956 | 5.557±3.277 | <0.001 | 0.001 | <0.001 |
| KISA | 162.297±679.62 | 275.438±1340.31 | 411.936±751.65 | <0.001 | NS | <0.001 |
| Elevation based | | | | | | |
| IHA | 5.628±4.396 | 12.877±9.562 | 32.064±24.694 | <0.001 | 0.014 | <0.001 |
| IHD | 0.009±0.005 | 0.024±0.017 | 0.107±0.057 | <0.001 | 0.034 | <0.001 |
| Pachymetric | | | | | | |
| TCP (μm) | 541.809±31.78 | 507.734±30.82 | 461.057±40.35 | <0.001 | <0.001 | <0.001 |
| $PPI_{max}$ | 1.287±0.204 | 1.658±0.415 | 2.710±0.835 | <0.001 | <0.001 | <0.001 |
| $ART_{max}$ | 432.971±78.40 | 327.253±90.67 | 187.129±64.320 | <0.001 | <0.001 | <0.001 |
| Integrated | | | | | | |
| BADD | 1.069±0.678 | 2.445±1.260 | 7.211±3.081 | <0.001 | <0.001 | <0.001 |
| PRFI | 0.105±0.100 | 0.536±0.345 | 0.955±0.962 | <0.001 | <0.001 | <0.001 |
| Sirius | | | | | | |
| Curvature based | | | | | | |
| K1 (D) | 42.156±4.891 | 42.950±1.652 | 45.274±2.508 | <0.001 | NS | <0.001 |
| K2 (D) | 44.612±2.930 | 44.458±1.821 | 48.257±3.023 | <0.001 | NS | <0.001 |
| Curve ($K_{max}$, D) | 45.425±2.098 | 46.619±2.213 | 54.118±4.406 | <0.001 | NS | <0.001 |
| SIf | 0.011±0.474 | 1.278±1.102 | 5.993±3.579 | <0.001 | 0.001 | <0.001 |
| SIb | 0.097±0.982 | 0.421±0.380 | 1.613±0.896 | <0.001 | 0.040 | <0.001 |
| Elevation based | | | | | | |
| KVf | 4.015±1.625 | 7.861±4.208 | 28.271±14.998 | <0.001 | 0.03 | <0.001 |
| KVb | 11.309±3.448 | 20.392±10.714 | 66.057±34.190 | <0.001 | 0.024 | <0.001 |
| Pachymetric | | | | | | |
| Thkmin (μm) | 539.221±32.953 | 501.127±32.421 | 445.219±86.449 | <0.001 | <0.001 | <0.001 |
| Corvis | | | | | | |
| Deformation | | | | | | |
| A1L (mm) | 2.407±0.292 | 2.220±0.332 | 2.107±0.353 | <0.001 | 0.002 | <0.001 |
| A2L (mm) | 2.063±0.391 | 1.868±0.288 | 1.660±0.339 | <0.001 | 0.002 | <0.001 |
| A1T (ms) | 7.595±0.468 | 7.255±0.506 | 6.965±0.424 | <0.001 | <0.001 | <0.001 |
| A2T (ms) | 21.041±0.385 | 21.171±0.425 | 21.386±0.462 | <0.001 | NS | <0.001 |
| A1V (mm/ms) | 0.118±0.015 | 0.128±0.019 | 0.140±0.027 | <0.001 | 0.015 | <0.001 |
| A2V (mm/ms) | -0.255±0.023 | -0.268±0.028 | -0.286±0.037 | <0.001 | 0.034 | <0.001 |
| DAratio1 | 1.572±0.050 | 1.618±0.066 | 1.688±0.082 | <0.001 | <0.001 | <0.001 |
| DAratio2 | 4.114±0.344 | 4.505±0.483 | 5.170±0.724 | <0.001 | <0.001 | <0.001 |
| HCDA (mm) | 0.942±0.079 | 0.991±0.105 | 1.055±0.115 | <0.001 | 0.012 | <0.001 |

**Table 2 Mean range of the studied parameters in normal, SKCN, and KCN eyes (continued)**

| Parameters | Normal | SKCN | KCN | *P* (ANOVA) | $P^1$ | $P^2$ |
|---|---|---|---|---|---|---|
| Deflection | | | | | | |
| A1DfA (mm) | 0.100±0.006 | 0.100±0.009 | 0.109±0.011 | <0.001 | NS | <0.001 |
| A2DfA (mm) | 0.110±0.011 | 0.108±0.014 | 0.118±0.013 | <0.001 | NS | <0.001 |
| HCDfA (mm) | 0.825±0.080 | 0.869±0.102 | 0.931±0.119 | <0.001 | 0.030 | <0.001 |
| $InvRad_{Max}$ (mm) | 0.159±0.016 | 0.172±0.020 | 0.199±0.031 | <0.001 | 0.002 | <0.001 |
| IntRC1($mm^{-1}$) | 6.873±0.834 | 7.759±1.278 | 9.508±2.027 | <0.001 | 0.001 | <0.001 |
| Integrated | | | | | | |
| ARTh | 519.448±138.67 | 403.783±122.3 | 229.875±92.76 | <0.001 | <0.001 | <0.001 |
| SPA1(mm Hg/mm) | 110.490±15.99 | 92.135±19.33 | 70.497±18.99 | <0.001 | <0.001 | <0.001 |
| CBI | 0.128±0.247 | 0.481±0.410 | 0.933±0.206 | <0.001 | <0.001 | <0.001 |
| TBI | 0.222±0.229 | 0.702±0.384 | 0.998±0.010 | <0.001 | <0.001 | <0.001 |

K1: Keratometry in flat meridian; K2: Keratometry in steep meridian; $K_{max}$: Max keratometry; ARC: Anterior radius of curvature in the 3 mm zone; PRC: Posterior radius of curvature in the 3.0 mm zone; TCP: Thinnest corneal point; $PPI_{max}$: Maximum of pachymetric progression index; $ART_{max}$: Maximum Ambrosio's relational thickness; ISV: Index of surface variance; IVA: Index of vertical asymmetry; KI: Keratoconus index; CKI: Central keratoconus index; IHA: Index of height asymmetry; IHD: Index of height decentration; I-S value: Inferior-superior difference value; KISA: Keratoconus percentage index; BADD: Belin/Ambrosio enhanced ectasia total deviation value; PRFI: Pentacam random forest index; ThkMin: Thinnest corneal thickness; SIf and SIb: Symmetry index of front and back of corneal curvature; KVf and KVb: Keratoconus vertex front/back; AL1, AL2: The length of flattened cornea at first/second applanations; A1T, A2T: Time from the beginning of air-puff until the first/second applanation; AV1, AV2: Corneal velocity at the first/second applanations; DAratio1, DAratio2: Maximum deformation amplitude ratio at 1 mm and 2 mm; HCDA: Deformation amplitude of the highest concavity; A1DfA, A2DfA: Deflection amplitude of the first/second applanation; HCDfA: Deflection amplitude of the highest concavity; $InvRad_{max}$: Maximum inverse radius; IntRC1: Integrated radiu; ARTh: Ambrosio relational thickness to the horizontal profile; SPA1: Stiffness parameter at first applanation; CBI: Corneal biomechanical index; TBI: Topographic and biomechanical index; SKCN: Subclinical keratoconus; KCN: Keratoconus; D: Diopter; NS: Not significant. [1]The comparison between normal and SKCN eyes; [2]The comparison between normal and KCN.

biomechanical parameters between SKCN and normal groups showed statistically significant differences for deformation and deflection parameters (except for A2T, A1DfA, and A2DfA) and all Corvis ST integrated indices ($P$<0.05).

In discriminating SKCN from normal eyes, Sirius SIb (sensitivity 86.2%, specificity 84.9%, AUC 0.908), and Pentacam I-S value (sensitivity 80%, specificity 79.2%, AUC 0.862) followed by Pentacam PRFI (sensitivity 71.1%, specificity 87.9%, AUC 0.847), and Corvis TBI (sensitivity 70.8%, specificity 83.0%, AUC 0.828) had the highest diagnostic ability (Delong, $P$>0.05; Tables 3 and 4).

The correlation analysis between parameters with the highest diagnostic ability showed that SIb, I-S value, PRFI, and TBI had a positive significant correlation with each other (all correlations were between 0.6 to 0.9, and $P$<0.001). There was a strong positive correlation between the PRFI and TBI ($r$=0.91, $P$<0.001).

ROC curves and dot plots of the best diagnostic parameters in keratoconic groups and normal group are shown in Figures 2 and 3.

Results of previous studies on parameters with the highest AUC using Pentacam, Sirius, and Corvis ST in KCN and SKCN groups are summarized in Table 5[5,8,18-29].

## DISCUSSION

This study analyzed topographic, tomographic, and biomechanical parameters derived from Pentacam, Sirius, and Corvis ST to identify the indices with the highest diagnostic ability for distinguishing clinical and subclinical forms of KCN.

With Pentacam, PRFI and IHD were the best indices for discriminating KCN from normal corneas, and PRFI and IS value had the highest AUC for discriminating SKCN from normal eyes. These results agree with the diagnostic ability of IHD in KCN cases reported by Huseynli *et al*[30] who found IHD with an AUC of 0.979 and cutoff of 0.013 followed by IHA were suitable indices for KCN detection. Similarly, Kovács *et al*[31] found IHD was more sensitive than BADD for differentiating KCN from normal eyes (AUC 0.97 *vs* 0.89). In contrast, Sedaghat *et al*[32] found that I-S value (AUC 0.986) had the highest ability among curvature parameters to discriminate KCN from normal eyes, while we found that IHD (AUC 0.999) had better accuracy than I-S value in KCN cases. These differences in the results may be due to the stage of KCN cases in research studies.

In the detection of SKCN, the Pentacam I-S value presented an AUC of 0.842 with 80.1% sensitivity and 79.2% specificity. Similarly, Bae *et al*[33] and Degirmenci *et al*[20] reported that

**Table 3 The result of ROC analysis to differentiate eyes with SKCN and KCN from normal eyes**

| Parameters | Normal *vs* SKCN | | | Normal *vs* KCN | | |
|---|---|---|---|---|---|---|
| | AUC | 95%CI | | AUC | 95%CI | |
| Pentacam | | | | | | |
| Front K1 (D) | 0.523 | 0.417 | 0.628 | 0.852 | 0.778 | 0.926 |
| Front K2 (D) | 0.502 | 0.396 | 0.608 | 0.919 | 0.866 | 0.972 |
| Front $K_{max}$ (D) | 0.619 | 0.518 | 0.720 | 0.991 | 0.980 | 1.000 |
| Back K1 (D) | 0.517 | 0.412 | 0.622 | 0.870 | 0.798 | 0.942 |
| Back K2 (D) | 0.516 | 0.412 | 0.621 | 0.916 | 0.861 | 0.971 |
| Back $K_{max}$ (mm) | 0.509 | 0.404 | 0.614 | 0.904 | 0.841 | 0.968 |
| ARC3 (mm) | 0.588 | 0.485 | 0.691 | 0.981 | 0.960 | 1.000 |
| PRC3 (mm) | 0.684 | 0.588 | 0.779 | 0.996 | 0.988 | 1.000 |
| ISV | 0.686 | 0.782 | 0.590 | 0.989 | 0.975 | 1.000 |
| IVA | 0.785 | 0.704 | 0.866 | 0.997 | 0.992 | 1.000 |
| KI | 0.813 | 0.736 | 0.889 | 0.997 | 0.991 | 1.000 |
| CKI | 0.503 | 0.398 | 0.608 | 0.887 | 0.811 | 0.964 |
| I-S value (D) | 0.862[a] | 0.798 | 0.927 | 0.991 | 0.980 | 1.000 |
| KISA | 0.546 | 0.451 | 0.641 | 0.795 | 0.679 | 0.850 |
| IHA | 0.719 | 0.627 | 0.810 | 0.879 | 0.813 | 0.946 |
| IHD | 0.792 | 0.710 | 0.873 | 0.9995[a] | 0.997 | 1.000 |
| TCP (μm) | 0.776 | 0.693 | 0.860 | 0.931 | 0.880 | 0.983 |
| $PPI_{max}$ | 0.802 | 0.724 | 0.881 | 0.987 | 0.970 | 1.000 |
| $ART_{max}$ | 0.825 | 0.751 | 0.899 | 0.989 | 0.974 | 1.000 |
| BADD | 0.842 | 0.773 | 0.912 | 0.9991 | 0.996 | 1.000 |
| PRFI | 0.847[a] | 0.783 | 0.911 | 1.000[a] | 0.999 | 1.000 |
| Sirius | | | | | | |
| K1 (D) | 0.563 | 0.459 | 0.667 | 0.861 | 0.789 | 0.932 |
| K2 (D) | 0.523 | 0.418 | 0.628 | 0.909 | 0.855 | 0.963 |
| Curve ($K_{max}$, D) | 0.687 | 0.592 | 0.783 | 0.985 | 0.969 | 1.000 |
| SIf | 0.877 | 0.814 | 0.939 | 0.995 | 0.986 | 1.000 |
| SIb | 0.908[a] | 0.851 | 0.965 | 0.981 | 0.945 | 1.000 |
| KVf | 0.826 | 0.752 | 0.899 | 0.993 | 0.983 | 1.000 |
| KVb | 0.812 | 0.736 | 0.889 | 0.999[a] | 0.996 | 1.000 |
| Thkmin (μm) | 0.790 | 0.709 | 0.871 | 0.930 | 0.879 | 0.981 |
| Corvis | | | | | | |
| A1L (mm) | 0.650 | 0.551 | 0.748 | 0.743 | 0.646 | 0.839 |
| A2L (mm) | 0.620 | 0.518 | 0.722 | 0.769 | 0.680 | 0.859 |
| A1T (ms) | 0.697 | 0.601 | 0.793 | 0.745 | 0.770 | 0.819 |
| A2T (ms) | 0.626 | 0.524 | 0.728 | 0.706 | 0.605 | 0.806 |
| A1V (mm/ms) | 0.655 | 0.557 | 0.754 | 0.738 | 0.641 | 0.834 |
| A2V (mm/ms) | 0.665 | 0.567 | 0.764 | 0.772 | 0.673 | 0.870 |
| DAratio1 | 0.725 | 0.632 | 0.817 | 0.911 | 0.854 | 0.967 |
| DAratio2 | 0.742 | 0.653 | 0.831 | 0.939 | 0.897 | 0.980 |
| HCDA (mm) | 0.666 | 0.566 | 0.765 | 0.769 | 0.677 | 0.861 |
| A1DfA (mm) | 0.505 | 0.400 | 0.609 | 0.774 | 0.679 | 0.869 |
| A2DfA (mm) | 0.502 | 0.396 | 0.607 | 0.695 | 0.593 | 0.797 |
| HCDfA (mm) | 0.655 | 0.555 | 0.754 | 0.763 | 0.669 | 0.857 |
| $InvRad_{max}$ (mm) | 0.698 | 0.602 | 0.793 | 0.901 | 0.840 | 0.962 |
| IntRC1 ($mm^{-1}$) | 0.728 | 0.636 | 0.821 | 0.931 | 0.881 | 0.981 |
| ARTh | 0.718 | 0.627 | 0.810 | 0.965 | 0.934 | 0.997 |
| SPA1 (mm Hg/mm) | 0.779 | 0.696 | 0.862 | 0.955 | 0.923 | 0.988 |
| CBI | 0.758 | 0.671 | 0.844 | 0.987 | 0.972 | 1.000 |
| TBI | 0.828[a] | 0.753 | 0.902 | 1.000[a] | 1.000 | 1.000 |

K1: Keratometry in flat meridian; K2: Keratometry in steep meridian; $K_{max}$: Max keratometry; ARC: Anterior radius of curvature in the 3 mm zone; PRC: Posterior radius of curvature in the 3.0 mm zone; TCP: Thinnest corneal point; $PPI_{max}$: Maximum of pachymetric progression index; $ART_{max}$: Maximum Ambrosio's relational thickness; ISV: Index of surface variance; IVA: Index of vertical asymmetry; KI: Keratoconus index; CKI: Central keratoconus index; IHA: Index of height asymmetry; IHD: Index of height decentration; I-S value: Inferior-superior difference value; KISA: Keratoconus percentage index; BADD: Belin/Ambrosio enhanced ectasia total deviation value; PRFI: Pentacam random forest index; ThkMin: Thinnest corneal thickness; SIf and SIb: Symmetry index of front and back of corneal curvature; KVf and KVb: Keratoconus vertex front/ back; AL1, AL2: The length of flattened cornea at first/second applanations; A1T, A2T: Time from the beginning of air-puff until the first/second applanation; AV1, AV2: Corneal velocity at the first/second applanations; DAratio1, DAratio2: Maximum deformation amplitude ratio at 1 mm and 2 mm; HCDA: Deformation amplitude of the highest concavity; A1DfA, A2DfA: Deflection amplitude of the first/second applanation; HCDfA: Deflection amplitude of the highest concavity; $InvRad_{max}$: Maximum inverse radius; IntRC1: Integrated radiu; ARTh: Ambrosio relational thickness to the horizontal profile; SPA1: Stiffness parameter at first applanation; CBI: Corneal biomechanical index; TBI: Topographic and biomechanical index; SKCN: Subclinical keratoconus; KCN: Keratoconus; D: Diopter. [a]The highest AUCs.

I-S value had higher AUC for detection of SKCN eyes than the other Pentacam topographic and topometric parameters (AUC 0.799 and 0.840, respectively). In contrast, Hashemi *et al*[34] determined IVA and ISV were higher in the SKCN eyes. This disparity could be explained by the different definitions of SKCN.

According to Lopes *et al*[19], who developed PRFI by machine learning techniques, this index can accurately identify patients who are at risk of ectasia in up to 80% of cases. In our study, PRFI provided slightly higher accuracy than IHD in KCN eyes and lower accuracy than I-S value in SKCN eyes. Similarly, Lopes *et al*[19] reported PRFI had higher AUC than IHD (AUC 1.00 versus 0.999) in patients with very asymmetric ectasia. However, they found PRFI had the highest diagnostic ability than I-S value (AUC 0.968 versus 0.635) in very asymmetric ectasia with normal topography eyes (VAE-NT). This finding has been confirmed by another study comparing the diagnostic ability of PRFI and I-S value (AUC 0.934 versus 0.677) in the VAE-NT group[35]. These different results can be attributed to the fact that the eyes in our SKCN group had subtle

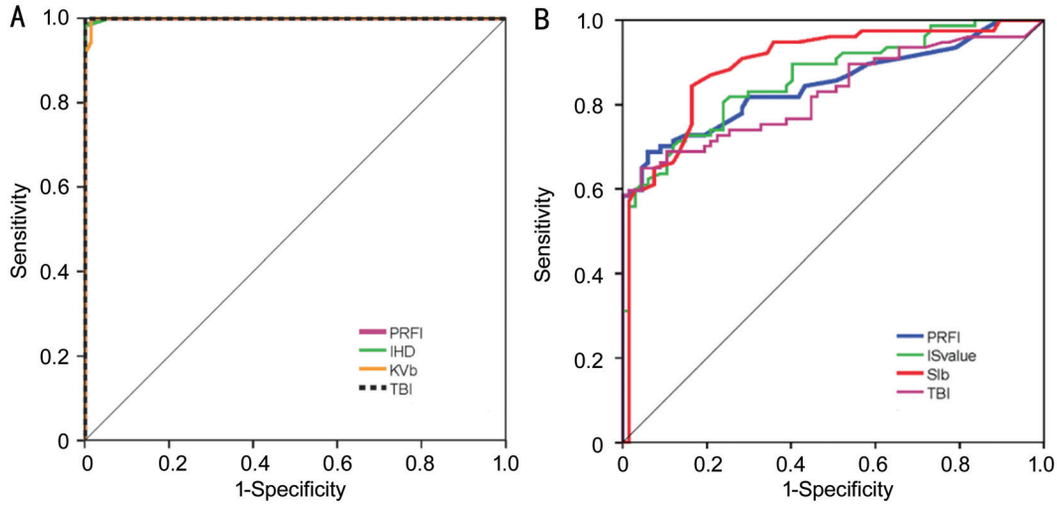


**Figure 2 ROC curves of Pentacam, Sirius and Corvis parameters with the highest AUCs to distinguish the KCN from normal eyes (A) and the SKCN from normal eyes (B).**

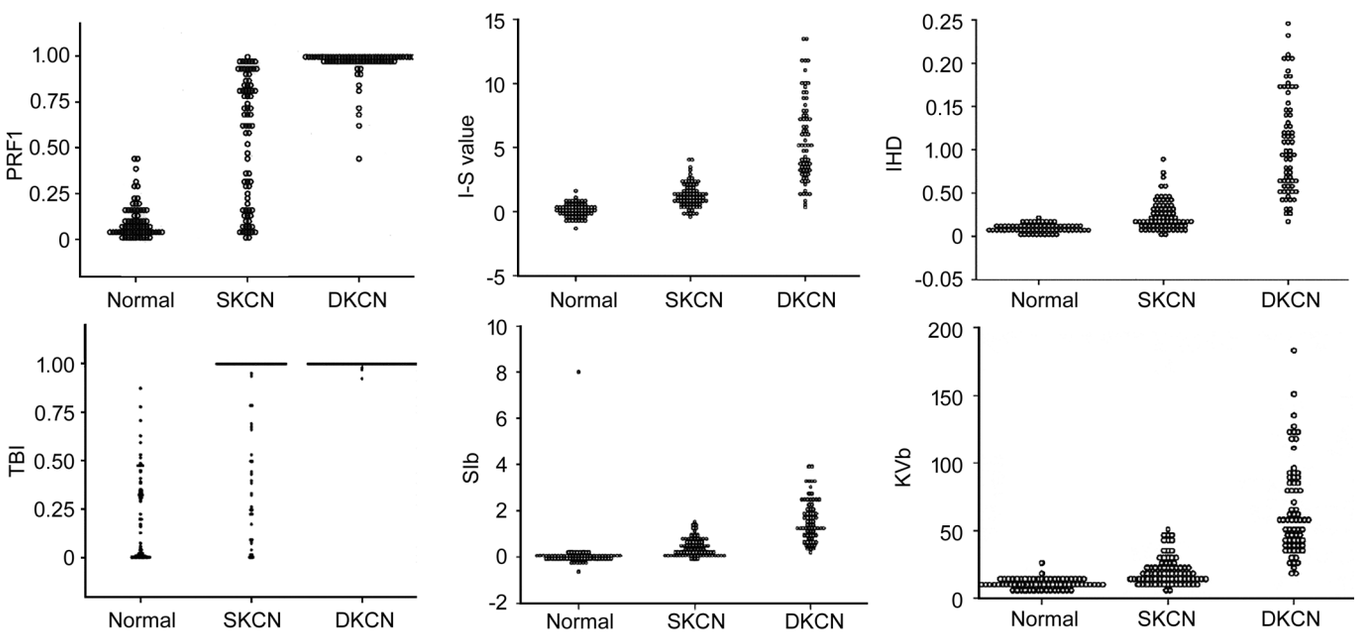


**Figure 3 Dots plot for Pentacam PRFI, I-S value, IHD, and Sirius SIb, KVb, and Corvis TBI.**

topographic abnormalities, however recent studies evaluate parameters in normal topography fellow eyes of KCN cases.

Another Pentacam topometric parameter is the KISA index which represents the asymmetry of the cornea and the details of its calculation have been previously described[36]. In our study, KISA index and keratometric parameters were not significantly different between the SKCN and normal groups. Studies have shown improved KISA accuracy when combined with tomography indices (e-KISA)[37] and wavefront indices (D-KISA)[38]. In the present study, although KISA appeared to be sufficiently powerful (AUC>0.8) for KCN diagnosis, it was not accurate enough for discriminating SKCN from normal eyes, which can be due to the lack of significant changes in astigmatism values and keratometric parameters (K values) in the early stages of the disease.

With Sirius, KVb (AUC 0.999) in the KCN group and SIb (AUC 0.908) in the SKCN group had the best discriminative ability from normal eyes. A few studies have investigated different parameters in Sirius. Vega-Estrada and Alio[22] assessed the posterior corneal indices in eyes with KCN and found a high discriminative ability for KVb (AUC 0.970). Shetty *et al*[5] reported root mean square per unit area (RMS/A) of Sirius was the best index to differentiate KCN from normal eyes (AUC 0.983), and RMS/A followed by SIb had the highest accuracy in SKCN eyes (AUC 0.692 and 0.612, respectively). They did not evaluate the keratoconus vertex index, and SKCN in their study was defined as the fellow eye of a patient with frank KCN, which differs from our criteria. Arbelaez *et al*[39] used a support vector machine (SVM) to develop a new classification method using a number

**Table 4 Cross-validation and diagnostic evaluation results**

| Parameters | Cross-validation | | | | | Diagnostic evaluation | | | | | |
|---|---|---|---|---|---|---|---|---|---|---|---|
| | Sensitivity | Specificity | LR+ | LR- | AUC | Sensitivity | Specificity | LR+ | LR- | AUC | Cutoff |
| Normal *vs* SKCN | | | | | | | | | | | |
| Pentacam | | | | | | | | | | | |
| I-S value | 80.6 | 73.08 | 3.00 | 0.27 | 0.863 | 80.1 | 79.2 | 3.84 | 0.25 | 0.862 | >0.44 |
| PRFI | 79.49 | 88.2 | 4.30 | 0.25 | 0.843 | 71.1 | 87.9 | 5.87 | 0.34 | 0.847 | >0.21 |
| Sirius | | | | | | | | | | | |
| SIb | 70.37 | 91.67 | 7.24 | 0.43 | 0.893 | 86.2 | 84.9 | 5.70 | 0.16 | 0.908 | >0.08 |
| Corvis | | | | | | | | | | | |
| TBI | 79.49 | 70.81 | 3.64 | 0.30 | 0.818 | 70.8 | 83 | 4.16 | 0.35 | 0.828 | >0.39 |
| Normal *vs* KCN | | | | | | | | | | | |
| Pentacam | | | | | | | | | | | |
| IHD | 90.01 | 100 | NA | 0.10 | 0.9995 | 98.6 | 100 | NA | 0.02 | 0.9995 | >0.02 |
| PRFI | 98.57 | 100 | NA | 0.01 | 0.9997 | 99.2 | 100 | NA | 0.01 | 1.000 | >0.53 |
| Sirius | | | | | | | | | | | |
| KVb | 92.57 | 100 | NA | 0.07 | 0.9989 | 100 | 98.5 | 53.00 | 0.00 | 0.9991 | >17.50 |
| Corvis | | | | | | | | | | | |
| TBI | 100 | 94.12 | 17.02 | 0.00 | 0.9998 | 100 | 100 | NA | 0.00 | 1.000 | >0.8 |

I-S value: Inferior-superior difference value; IHD: Index of height decentration; PRFI: Pentacam random forest index; SIb: Symmetry index of back of corneal curvature; KVb: Keratoconus vertex back; TBI: Topographic and biomechanical index; LR±: Positive/negative likelihood ratio; NA: Not available (could not be calculated); AUC: Area under the curve.

**Table 5 Summary of previous reports for distinguishing clinical and SKCN from normal eyes**

| Author | Year | Device | Indices | Cutoff | AUC | Sensitivity | Specificity |
|---|---|---|---|---|---|---|---|
| KCN *vs* Normal | | | | | | | |
| Sedghipour *et al*[18] | 2012 | Pentacam | KISA | - | - | 0.96 | 100 |
| Shetty *et al*[5] | 2017 | Pentacam | BADD | 2.6 | 0.972 | 1.00 | 0.614 |
| Lopes *et al*[19] | 2018 | Pentacam | PRFI | 0.52 | 1.00 | 100 | 0.966 |
| Degirmenci *et al*[20] | 2018 | Pentacam | $CT_{min}$ | 0.85 | 491.5 | 0.87 | 0.73 |
| Hashemi *et al*[21] | 2019 | Pentacam | IVA | 0.20 | 0.952 | 0.875 | 0.963 |
| Vega-Estrada *et al*[22] | 2019 | Sirius | KVb | 13.5 | - | 0.890 | 0.840 |
| Tian *et al*[8] | 2014 | Corvis | DA | - | 0.882 | 0.817 | - |
| Chan *et al*[23] | 2017 | Corvis | $InvRad_{max}$ | 0.19 | 0.954 | 0.81 | 0.87 |
| Ferreira-Mendes *et al*[24] | 2019 | Corvis | TBI | 0.385 | 0.99 | 97.1 | 98.1 |
| SKCN *vs* Normal | | | | | | | |
| Ucakhan *et al*[25] | 2011 | Pentacam | PPIave | 1.15 | 0.84 | 0.818 | 0.788 |
| Lopes *et al*[19] | 2018 | Pentacam | PRFI | 0.125 | 0.968 | 0.852 | 0.966 |
| Degirmenci *et al*[20] | 2018 | Pentacam | ISV | 18.5 | 0.88 | 0.80 | 0.80 |
| Song *et al*[26] | 2019 | Pentacam | BADD | 1.2 | 0.799 | 63.64 | 85.71 |
| Heidari *et al*[27] | 2020 | Sirius | BCVf | 0.245 | 0.877 | 87.7 | 83 |
| Shetty *et al*[5] | 2019 | Sirius | RMS/A | 0.088 | 0.730 | 0.108 | 0.719 |
| Wang *et al*[28] | 2017 | Corvis | CBI | 0.215 | 0.785 | 80.3 | 63.2 |
| Chan *et al*[29] | 2018 | Corvis | TBI | 0.16 | 0.925 | 0.844 | 0.824 |

KCN: Keratoconus; SKCN: Subclinical keratoconus; KISA: KCN percentage index; BADD: Belin/Ambrosio enhanced ectasia total derivation value; PRFI: Pentacam random forest index; $CT_{min}$: Minimum corneal thickness; IVA: Index of vertical asymmetry; KVb: Keratoconus vertex back; DA: Deformation amplitude; $InvRad_{max}$: Maximum inverse radius; PPIave: Average of pachymetric progression index; ISV: Index of surface variance; BCVf: Front Baiocchi-Calossi-Versaci; RMS/A: Root mean square per unit area; TBI: Topographic and biomechanical index; CBI: Corneal biomechanical index; SKCN: Subclinical keratoconus; AUC: Area under the curve.

of topographic and tomographic indices in Sirius, and they concluded that adding posterior corneal surface data improved the accuracy, especially for SKCN. However, the diagnostic ability of individual indices were not reported.

The outcomes of our study indicate posterior and anterior curvature-based indices such as SIb (AUC 0.908) and I-S value (AUC 0.862) as topographic asymmetric parameters have a better ability to detect early forms of KCN compared with elevation-based and pachymetric parameters. These findings are compatible with Bae *et al*[33] study who reported that curvature data are more accurate than pachymetric and elevation parameters for early detection of KCN. Our study showed a high diagnostic ability of SIb index to demonstrate changes of the symmetry in the posterior surface of the cornea and highlights early alteration in the posterior surface of the cornea in the early stage of the ectasia. Similarly, KVb with a perfect AUC as a posterior corneal vertex elevation was one of the sensitive variables when comparing normal and definite cases of KCN. These results are consistent with other studies that found posterior corneal surface are useful to distinguish normal corneas from keratoconic corneas as the first indicator of ectasia[40-41].

Assessment of the biomechanical parameters using the Corvis ST showed that TBI had the best discriminative ability compared with other parameters for differentiating both SKCN and KCN from normal eyes. TBI is combined with corneal tomography and biomechanical data and is claimed to be highly sensitive for the diagnosis of SKCN in patients with normal topography[9]. The cutoff value of this parameter in the KCN group in our study was (0.80) with 100% sensitivity and specificity, which was similar to the cutoff points reported by Ambrósio *et al*[9] (0.79) and Steinberg *et al*[42] (0.75) with 100%sensitivity and specificity in both studies. However, in the SKCN group of our study, the cutoff point for TBI was 0.39 with a sensitivity of 70.8% and a specificity of 83%, which is different from what Ambrósio *et al*[9] reported (cutoff point of 0.29, sensitivity 90% and specificity 96%). In a recent study, Koc *et al*[43] reported a similar cutoff value (0.29) with lower accuracy (sensitivity 67% and specificity 86%) in the SKCN group. The difference in cutoff points could be due to differences in patient selection.

This study showed that both posterior and anterior curvature-based changes can detect SKCN earlier than biomechanical analysis which is similar to the studies claiming that biomechanical properties alone may not be sufficient for detecting subclinical forms of ectatic disorders[43-44]. This may be explained by the role of later changes in corneal thickness in the course of the disease and its fundamental role on biomechanical indices which is not evident in the early stages of the disease, however with further development of the ectasia the biomechanical instability of the cornea and therefore the diagnostic power of biomechanical indices increases. However, they can be applied with caution as additional axillary diagnostic tools for detecting ectasia in some clinical states as adjutant modalities.

The correlation analysis showed that the best diagnostic parameters with the three devices were moderately to strongly correlated with each other. KVb and IHD, which are both related to corneal height, were highly correlated with each other in the KCN group, and PRFI and TBI, which are partly based on corneal tomography data, had a strong correlation with each other in both KCN and SKCN groups. These findings suggest that these parameters with high accuracy and high level of relationship, can play a significant role in distinguishing keratoconic from normal corneas.

In conclusion, our study demonstrated acceptable discrimination ability for all topographic, tomographic, and integrated biomechanical indices in differentiating clinical KCN from normal eyes. However, both posterior and anterior curvature-based parameters including SIb of Sirius and IS value of Pentacam followed by integrated indices such as PRFI of Pentacam and TBI of Corvis were the most powerful indices to detect early KCN, respectively. We suggest both tomographic and biomechanical assessments as complementary diagnostic methods for early diagnosis of ectatic corneal disorders.

**ACKNOWLEDGEMENTS**

**Conflicts of Interest: Heidari Z,** None; **Hashemi H,** None; **Mohammadpour M,** None; **Amanzadeh K,** None; **Fotouhi A,** None.

**REFERENCES**

1 Ambrósio R Jr, Randleman JB. Screening for ectasia risk: what are we screening for and how should we screen for it? *J Refract Surg* 2013;29(4):230-232.

2 Mohammadpour M, Heidari Z, Hashemi H. Updates on managements for keratoconus. *J Curr Ophthalmol* 2018;30(2):110-124.

3 De la Parra-Colín P, Garza-León M, Barrientos-Gutierrez T. Repeatability and comparability of anterior segment biometry obtained by the Sirius and the Pentacam analyzers. *Int Ophthalmol* 2014;34(1):27-33.

4 Shetty R, Arora V, Jayadev C, Nuijts RM, Kumar M, Puttaiah NK, Kummelil MK. Repeatability and agreement of three Scheimpflug-based imaging systems for measuring anterior segment parameters in keratoconus. *Invest Ophthalmol Vis Sci* 2014;55(8):5263-5268.

5 Shetty R, Rao H, Khamar P, Sainani K, Vunnava K, Jayadev C, Kaweri L. Keratoconus screening indices and their diagnostic ability to distinguish normal from ectatic corneas. *Am J Ophthalmol* 2017;181:140-148.

6 Vinciguerra R, Ambrósio R Jr, Elsheikh A, Roberts CJ, Lopes B, Morenghi E, Azzolini C, Vinciguerra P. Detection of keratoconus with a new biomechanical index. *J Refract Surg* 2016;32(12):803-810.

7 Hernández-Camarena JC, Chirinos-Saldaña P, Navas A, Ramirez-Miranda A, de la Mota A, Jimenez-Corona A, Graue-Hernindez EO.

Repeatability, reproducibility, and agreement between three different Scheimpflug systems in measuring corneal and anterior segment biometry. *J Refract Surg* 2014;30(9):616-621.

8 Tian L, Huang YF, Wang LQ, Bai H, Wang Q, Jiang JJ, Wu Y, Gao M. Corneal biomechanical assessment using corneal visualization scheimpflug technology in keratoconic and normal eyes. *J Ophthalmol* 2014;2014:147516.

9 Ambrósio R Jr, Lopes BT, Faria-Correia F, Salomão MQ, Bühren J, Roberts CJ, Elsheikh A, Vinciguerra R, Vinciguerra P. Integration of scheimpflug-based corneal tomography and biomechanical assessments for enhancing ectasia detection. *J Refract Surg* 2017;33(7):434-443.

10 Roberts CJ, Mahmoud AM, Bons JP, Hossain A, Elsheikh A, Vinciguerra R, Vinciguerra P, Ambrósio R Jr. Introduction of two novel stiffness parameters and interpretation of air puff-induced biomechanical deformation parameters with a dynamic scheimpflug analyzer. *J Refract Surg* 2017;33(4):266-273.

11 Rabinowitz YS. Keratoconus. *Surv Ophthalmol* 1998;42(4):297-319.

12 Rabinowitz YS, McDonnell PJ. Computer-assisted corneal topography in keratoconus. *Refract Corneal Surg* 1989;5(6):400-408.

13 Motlagh MN, Moshirfar M, Murri MS, Skanchy DF, Momeni-Moghaddam H, Ronquillo YC, Hoopes PC. Pentacam® corneal tomography for screening of refractive surgery candidates: a review of the literature, part I. *Med Hypothesis Discov Innov Ophthalmol* 2019;8(3):177-203.

14 Henriquez MA, Hadid M, Izquierdo L Jr. A systematic review of subclinical keratoconus and forme fruste keratoconus. *J Refract Surg* 2020;36(4):270-279.

15 Yang KL, Xu LY, Fan Q, Zhao DQ, Ren SW. Repeatability and comparison of new Corvis ST parameters in normal and keratoconus eyes. *Sci Rep* 2019;9(1):15379.

16 Lopes BT, Ramos IdC, Salomão MQ, Canedo ALC, Ambrósio Jr R. Perfil paquimétrico horizontal para a detecção do ceratocone. *Rev Bras Oftalmol* 2015;74(6):382-385.

17 DeLong ER, DeLong DM, Clarke-Pearson DL. Comparing the areas under two or more correlated receiver operating characteristic curves: a nonparametric approach. *Biometrics* 1988;44(3):837.

18 Sedghipour MR, Sadigh AL, Motlagh BF. Revisiting corneal topography for the diagnosis of keratoconus: use of Rabinowitz's KISA% index. *Clin Ophthalmol* 2012;6:181-184.

19 Lopes BT, Ramos IC, Salomão MQ, Guerra FP, Schallhorn SC, Schallhorn JM, Vinciguerra R, Vinciguerra P, Price FW Jr, Price MO, Reinstein DZ, Archer TJ, Belin MW, Machado AP, Ambrósio R Jr. Enhanced tomographic assessment to detect corneal ectasia based on artificial intelligence. *Am J Ophthalmol* 2018;195:223-232.

20 Değirmenci C, Palamar M, İsmayilova N, Eğrilmez S, Yağcı A. Topographic evaluation of unilateral keratoconus patients. *Turk J Ophthalmol* 2019;49(3):117-122.

21 Hashemi H, Khabazkhoob M, Pakzad R, Bakhshi S, Ostadimoghaddam H, Asaharlous A, Yekta R, Aghamirsalim M, Yekta A. Pentacam accuracy in discriminating keratoconus from normal corneas: a diagnostic evaluation study. *Eye Contact Lens* 2019;45(1):46-50.

22 Vega-Estrada A, Alio JL. Keratoconus corneal posterior surface characterization according to the degree of visual limitation. *Cornea* 2019;38(6):730-736.

23 Chan TC, Wang YM, Yu M, Jhanji V. Comparison of corneal dynamic parameters and tomographic measurements using Scheimpflug imaging in keratoconus. *Br J Ophthalmol* 2018;102(1):42-47.

24 Ferreira-Mendes J, Lopes BT, Faria-Correia F, Salomão MQ, Rodrigues-Barros S, Ambrósio R Jr. Enhanced ectasia detection using corneal tomography and biomechanics. *Am J Ophthalmol* 2019;197:7-16.

25 Uçakhan ÖÖ, Cetinkor V, Özkan M, Kanpolat A. Evaluation of Scheimpflug imaging parameters in subclinical keratoconus, keratoconus, and normal eyes. *J Cataract Refract Surg* 2011;37(6):1116-1124.

26 Song P, Yang KL, Li P, Liu Y, Liang DF, Ren SW, Zeng QY. Assessment of corneal pachymetry distribution and morphologic changes in subclinical keratoconus with normal biomechanics. *Biomed Res Int* 2019;2019:1748579.

27 Heidari Z, Mohammadpour M, Hashemi H, Jafarzadehpur E, Moghaddasi A, Yaseri M, Fotouhi A. Early diagnosis of subclinical keratoconus by wavefront parameters using Scheimpflug, Placido and Hartmann-Shack based devices. *Int Ophthalmol* 2020;40(7):1659-1671.

28 Wang YM, Chan TCY, Yu M, Jhanji V. Comparison of corneal dynamic and tomographic analysis in normal, forme fruste keratoconic, and keratoconic eyes. *J Refract Surg* 2017;33(9):632-638.

29 Chan TCY, Wang YM, Yu M, Jhanji V. Comparison of corneal tomography and a new combined tomographic biomechanical index in subclinical keratoconus. *J Refract Surg* 2018;34(9):616-621.

30 Huseynli S, Abdulaliyeva F. Evaluation of scheimpflug tomography parameters in subclinical keratoconus, clinical keratoconus and normal Caucasian eyes. *Turk J Ophthalmol* 2018;48(3):99-108.

31 Kovács I, Miháltz K, Kránitz K, Juhász É, Takács Á, Dienes L, Gergely R, Nagy ZZ. Accuracy of machine learning classifiers using bilateral data from a Scheimpflug camera for identifying eyes with preclinical signs of keratoconus. *J Cataract Refract Surg* 2016;42(2):275-283.

32 Sedaghat MR, Momeni-Moghaddam H, Ambrósio R Jr, Heidari HR, Maddah N, Danesh Z, Sabzi F. Diagnostic ability of corneal shape and biomechanical parameters for detecting frank keratoconus. *Cornea* 2018;37(8):1025-1034.

33 Bae GH, Kim JR, Kim CH, Lim DH, Chung ES, Chung TY. Corneal topographic and tomographic analysis of fellow eyes in unilateral keratoconus patients using Pentacam. *Am J Ophthalmol* 2014;157(1):103-109.e1.

34 Hashemi H, Beiranvand A, Yekta A, Maleki A, Yazdani N, Khabazkhoob M. Pentacam top indices for diagnosing subclinical and definite keratoconus. *J Curr Ophthalmol* 2016;28(1):21-26.

35 Salomão MQ, Hofling-Lima AL, Gomes Esporcatte LP, Lopes B, Vinciguerra R, Vinciguerra P, Bühren J, Sena N Jr, Luz Hilgert GS,

Ambrósio R Jr. The role of corneal biomechanics for the evaluation of ectasia patients. *Int J Environ Res Public Health* 2020;17(6):E2113.

36 Rabinowitz YS, Rasheed K. KISA% index: a quantitative videokeratography algorithm embodying minimal topographic criteria for diagnosing keratoconus. *J Cataract Refract Surg* 1999;25(10): 1327-1335.

37 Bühren J, Kook D, Kohnen T. Suitability of various topographic corneal parameters for diagnosis of early keratoconus. *Ophthalmologe* 2012;109(1):37-44.

38 Steinberg J, Aubke-Schultz S, Frings A, Hülle J, Druchkiv V, Richard G, Katz T, Linke SJ. Correlation of the KISA% index and Scheimpflug tomography in 'normal', 'subclinical', 'keratoconus-suspect' and 'clinically manifest' keratoconus eyes. *Acta Ophthalmol* 2015;93(3):e199-e207.

39 Arbelaez MC, Versaci F, Vestri G, Barboni P, Savini G. Use of a support vector machine for keratoconus and subclinical keratoconus detection by topographic and tomographic data. *Ophthalmology* 2012;119(11):2231-2238.

40 Du XL, Chen M, Xie LX. Correlation of basic indicators with stages of keratoconus assessed by Pentacam tomography. *Int J Ophthalmol* 2015;8(6):1136-1140.

41 Safarzadeh M, Nasiri N. Anterior segment characteristics in normal and keratoconus eyes evaluated with a combined Scheimpflug/Placido corneal imaging device. *J Curr Ophthalmol* 2016;28(3):106-111.

42 Steinberg J, Siebert M, Katz T, Frings A, Mehlan J, Druchkiv V, Bühren J, Linke SJ. Tomographic and biomechanical scheimpflug imaging for keratoconus characterization: a validation of current indices. *J Refract Surg* 2018;34(12):840-847.

43 Koc M, Aydemir E, Tekin K, Inanc M, Kosekahya P, Kiziltoprak H. Biomechanical analysis of subclinical keratoconus with normal topographic, topometric, and tomographic findings. *J Refract Surg* 2019;35(4):247-252.

44 Mohammadpour M, Etesami I, Yavari Z, Naderan M, Abdollahinia F, Jabbarvand M. Ocular response analyzer parameters in healthy, keratoconus suspect and manifest keratoconus eyes. *Oman J Ophthalmol* 2015;8(2):102-106.